

MMIC-to-Waveguide Transition at 160 GHz with Galvanic Isolation

Martin Hitzler*, Stefan Saulig*, Linus Boehm*, Winfried Mayer†, and Christian Waldschmidt*

*Institute of Microwave Techniques, University of Ulm, 89081 Ulm, Germany, Email: martin.hitzler@uni-ulm.de

†Endress & Hauser GmbH + Co. KG, 79689 Maulburg, Germany

Abstract—In this paper a new approach for a monolithic microwave integrated circuit (MMIC) to rectangular waveguide transition is presented, which has no need for a specific package. The transition uses a partly integrated antenna with a patch radiator and a tapered dielectric waveguide to guide the wave into a widened metallic waveguide. Due to the usage of the dielectric waveguide the ground potentials of the MMIC and the metallic waveguide are galvanically isolated. The proposed transition was characterized in back-to-back measurements without probe-tips. A minimum insertion loss of 3 dB was measured. To the author's knowledge, this is the first approach of a galvanically isolated MMIC to metallic waveguide transition.

Index Terms—MMIC to waveguide transition, chip to waveguide transition, MMIC, dielectric waveguide, rectangular waveguide, galvanic isolation.

I. INTRODUCTION

Increasing transistor speeds in low-cost semiconductor technologies, like Silicon-Germanium (SiGe) and CMOS, enable applications at 60 GHz for WLAN and 79 GHz for driver assistance systems. Above 100 GHz, the ISM bands at 120 GHz and 240 GHz are frequently used for demonstrators. Besides the MMIC, its packaging is a crucial point for the performance of the system. For many tasks, a standard connection of the sensor to the outside world is advantageous or necessary. Thus, an MMIC to waveguide transition is required.

In the literature, the package is often used to realize the transition to rectangular waveguide. In [1], a low-loss transition in the redistribution layer of an eWLB package is discussed. An approach with a packaged antenna in the redistribution layer of the eWLB package is demonstrated in [2]. Recently, [3] presented an MMIC to rectangular waveguide transition at 60 GHz with losses of 2.5 dB by using PCB technology. The disadvantage of all the mentioned approaches is the need for a specific RF package or PCB technology. [4] realized an integrated antenna based on a dielectric resonator, which is surrounded by a tapered horn antenna guiding to a rectangular waveguide. This approach avoids a transition via a package or PCB but gives almost no space for die bonding.

In this paper, a transition is presented, which guides the electromagnetic wave directly from the MMIC via a dielectric waveguide section to the metallic waveguide. Consequently, a direct die attachment on PCB as well as an open QFN standard package can be utilized, which results in lower costs and shorter design processes compared to eWLB package. Additionally, a galvanic isolation is achieved by using a dielectric waveguide. Due to the non-resonant behavior of the dielectric waveguide its length can be almost arbitrary so that the distance between MMIC and rectangular waveguide is adjustable.

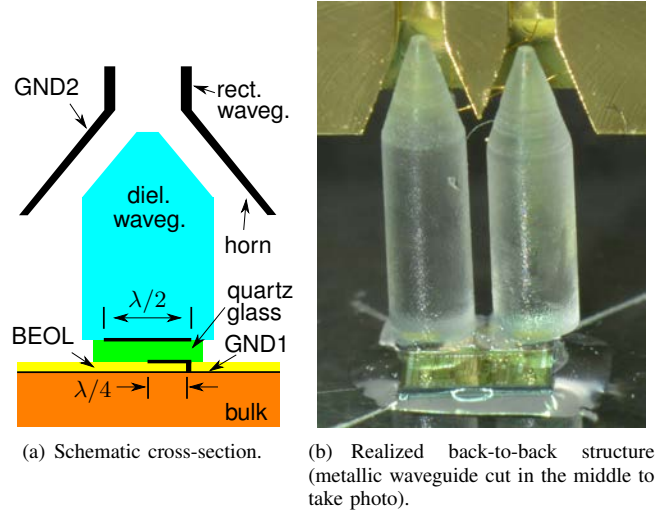


Fig. 1. MMIC to rectangular waveguide transition.

In this paper, Section II describes the principle of the transition and Section III explains the assembly. The challenges and results of the back-to-back measurements are shown in Section IV.

II. TRANSITION PRINCIPLE

The transition is composed of a partly integrated antenna to couple efficiently from MMIC into the dielectric waveguide, which guides the wave to a widened rectangular waveguide. The schematic cross-section of the proposed structure is depicted in Fig. 1(a). First, the structure from MMIC to dielectric waveguide is explained.

A. From MMIC to Dielectric Waveguide

The transition from the MMIC to the dielectric waveguide consists of three parts as depicted in Fig 2. The first part is a shorted $\lambda/4$ patch, which is integrated in the SiO₂ back end of line (BEOL) of the MMIC as wave launching or coupling structure, known from an 80 GHz version in [5] or [6]. The second part is a $\lambda/2$ patch radiator on a 127 μm thick quartz glass carrier, as in [7]. This metallized quartz glass is mounted on the MMIC above the coupling structure so that the red crosses in Fig. 2 are aligned in z-direction. GND1 is the ground potential of the shorted $\lambda/4$ patch and the overlying radiating $\lambda/2$ patch on the quartz glass. The third part is the dielectric waveguide, which is fixed on top of the patch radiator to guide the wave towards the rectangular waveguide without conductive material. PMMA with a permittivity of about 2.3 was used as prototyping material for the dielectric waveguide.

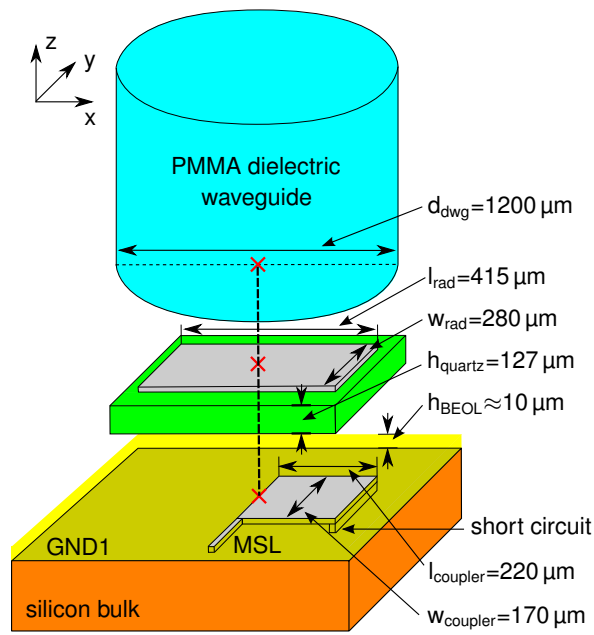


Fig. 2. Perspective schematic view of the transition from MMIC to dielectric waveguide with dimensions.

The operating frequency band is mainly adjusted by the length of the radiating patch. The coupling between the MMIC and the patch radiator and thus the impedance matching depends on the thickness of the quartz glass h_{quartz} , the width of the patch radiator w_{rad} and the dimensions l_{coupler} and w_{coupler} of the shorted coupling patch on the MMIC. Due to the back-to-back measurement setup, which is explained in Section IV, the maximum diameter of the cylindrical waveguide was chosen to 1.2 mm to achieve a distance between the dielectric waveguides of at least $400\mu\text{m}$. The distance between the chip surface and the horn region was fixed to 3 mm. With these boundary conditions the size of the shorted $\lambda/4$ patch was optimized to $220\mu\text{m} \times 170\mu\text{m}$ and the patch radiator was optimized to $415\mu\text{m} \times 280\mu\text{m}$.

In order to assess the loss mechanisms two different cases were simulated and depicted in Fig. 3. The dashed curves show the S-Parameters, which contain only parasitic radiation, the solid curves include additionally material and conductivity losses. Minimum radiation losses of 1.7 dB are obtained from the transmission curve (---). The difference between the two transmission coefficients of approximately 2 dB indicates the additional losses due to limited conductivity and material losses in the back end of the MMIC. When taking the losses into account, a minimum insertion loss of 3.8 dB is achieved. The resonant behavior of the patch limits the bandwidth to 33 GHz, or 20%, when referring to the 3 dB decline from the maximum transmission value.

B. From Dielectric Waveguide to Metallic Waveguide

The second step of the transition can be designed completely non-resonant. In [8], an approach is discussed, in which the

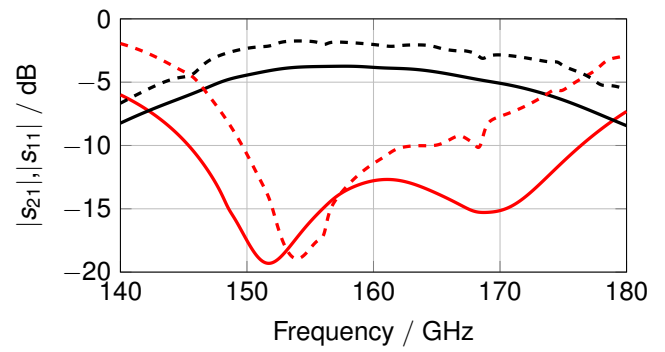


Fig. 3. Simulated transmission (black) and reflection (red) coefficients of the transition from MMIC to dielectric waveguide with radiation losses only (dashed) and including additionally the antenna-on-chip efficiency (solid).

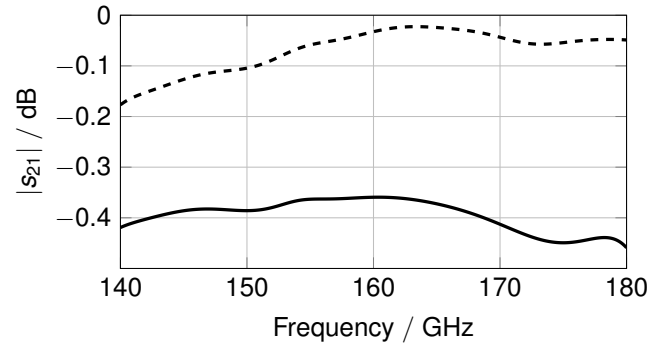


Fig. 4. Simulated transmission coefficient of the transition from dielectric to metallic waveguide for radiation losses only (---) and including all types of losses (—).

tapered dielectric waveguide is pressed between two metallic waveguide half shells. For the assembly, a mechanical decoupling between die and metallic waveguide has several advantages. First, mechanical tensions on the metallic waveguide or thermal expansions do not stress the die. Second, the chain of tolerances is interrupted since the metallic waveguide can be positioned relatively to the dielectric waveguide. By positioning the tapered dielectric waveguide in the horn region of the metallic waveguide, as depicted in Fig. 1, a simple way for decoupling the two parts is created. The highest transmission and lowest reflection is achieved when the tapering angles of the two waveguides are identical in the E-plane, depicted as xz-plane in Fig. 5. The length of the horn was 3.4 mm in z-direction with a taper angle of 20° in the E-plane and 28° in the H-plane. The cylindrical taper of the dielectric waveguide was simulated with a height of 1.5 mm and an angle of 20° . The simulated transmission coefficients for the lossless and lossy case are shown in Fig. 4. The losses in the lossless case for lower frequencies are due to larger stray fields in the vicinity of the dielectric waveguide, which radiate into free space at the transition. In the lossy case a comparably flat insertion loss curve with a minimum of 0.36 dB was simulated. The matching is better than 20 dB in the whole band for both cases.

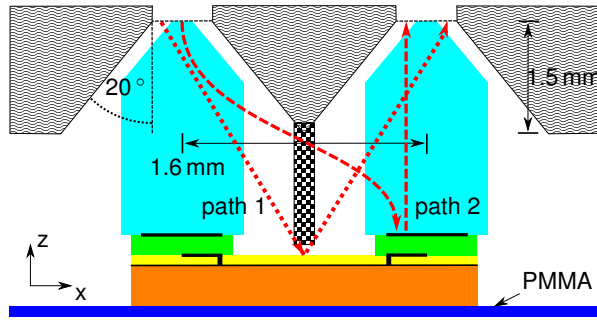


Fig. 5. Schematic cross-section of the back-to-back structure with dimensions and metal wall between the dielectric waveguides for crosstalk suppression.

III. REALIZATION OF THE STRUCTURE

The characterization of the proposed transition is challenging. A direct measurement with a probe tip on one side and a rectangular waveguide flange on the other side is not possible because the mounting of the widened rectangular waveguide above the die would hide the pad for probing. Hence rectangular waveguide flanges are used for the back-to-back measurements. Consequently, a SiGe BEOL MMIC was fabricated, which contains two shorted $\lambda/4$ patches separated by 1.6 mm, as shown in Fig. 5. Consequently, the remaining distance between the dielectric waveguides is only approximately 400 μm . The two coupling patches on the MMIC were connected with a microstrip line.

In the first step of the assembly the MMIC is glued with epoxy adhesive on a PMMA bottom plate. Subsequently, the quartz glasses are glued on top of the die. The dielectric waveguides are fixed with petrolatum above the quartz glasses for prototyping flexibility, reusability and positioning purposes. In a mature process petrolatum can be substituted with epoxy adhesive. The realization of the whole transition is illustrated in Fig. 1(b).

The rectangular waveguide component consists of two parts. The upper part is a measurement adapter to access the two parallel rectangular waveguides. The lower part contains the two horn regions and two short, parallel rectangular waveguides. Because of the limited distance between the integrated coupling structures, the horn region of the rectangular waveguides had to be shortened to 1.5 mm in the z-direction as shown in Fig. 5. Both components are composed by two half shells. A PVC frame was used as spacer between the PMMA bottom plate and the metallic waveguide component.

The positioning can be executed with a microscope by moving the rectangular waveguide on the spacer frame in the xy-plane until the center of the dielectric waveguides coincides with the center of the rectangular waveguides. The tolerances are about $\pm 50 \mu\text{m}$. Due to the transparency of the PMMA bottom plate, the structure can be additionally turned upside down and positioned from underneath even without microscope.

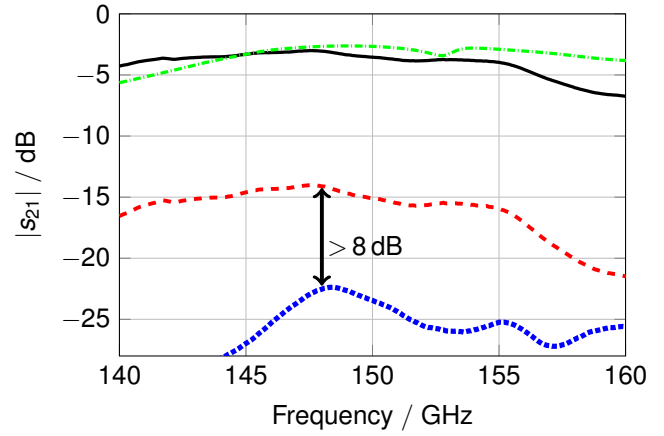


Fig. 6. Measured transmission coefficient of the back-to-back setup (---). Same measurement but with cut microstrip line on the MMIC (.....). Measured one-way transmission coefficient calculated from the back-to-back measurement (—), simulated one-way transmission coefficient including epoxy adhesive and petrolatum (-.-.-).

IV. MEASUREMENT RESULTS

For the back-to-back measurements, two crucial parasitic paths must be attenuated. First, the parasitic reflections on the $2 \text{ mm} \times 1.5 \text{ mm}$ die surface disturb the transmission measurement, illustrated as path 1 in Fig. 5. Second, the crosstalk, due to the coupling of one dielectric waveguide to the adjacent one, guides a part of the wave to the right patch. For frequencies, where the patch radiator is non-resonant, this incident wave is reflected and guided to the right metallic waveguide depicted as path 2 in Fig. 5. To suppress these two paths a metal wall was added between the two dielectric waveguides as drawn in Fig. 5 (chess pattern).

The transmission coefficient of the back-to-back structure with metal wall is shown in Fig. 6 as (---). For comparison, the transmission coefficient of a transition with a cut microstrip line on the MMIC is illustrated as (.....). The cut was achieved by focused-ion-beam (FIB) technology. The insertion loss difference of 8 dB between the complete and the cut transition validates that the guiding of the electromagnetic wave on the microstrip line of the MMIC is the dominant transmission path between the two metallic waveguides. The minimum insertion loss of the back-to-back structure is 14 dB. For the microstrip line, which connects the two shorted $\lambda/4$ patches, an insertion loss of 2 dB is subtracted, which was measured with a test microstrip line on another BEOL chip. This decreases the minimum back-to-back insertion loss to 12 dB. Under the assumption of a matched transition in the frequency range of maximum transmission the minimum insertion loss of the one-way transition is 6 dB (12 dB/2).

In Section II-A a degradation of about 2 dB is simulated due to the limited efficiency of the integrated antenna. The state-of-the-art of measured integrated antenna efficiency is about 50% or -3 dB, as in [5] or [7]. Referring to the state-of-the-art, the insertion loss of the transition without losses due to limited antenna efficiency can be approximated by a 3 dB

lower value. Removing this 3 dB from the one-way insertion loss results in (—) in Fig. 6. The minimum loss of 3 dB is 0.5 dB higher than the simulated loss without antenna losses (---). The measured transmission coefficient is shifted about 5 GHz to lower frequencies probably due to additional epoxy adhesive and petrolatum around the quartz glass, which would increase the effective permittivity of the patch resonator.

V. SUMMARY

This paper presents for the first time a transition from MMIC to rectangular waveguide with galvanic isolation. This is achieved by a dielectric waveguide as connecting element. The structure from MMIC via dielectric waveguide into the rectangular waveguide is discussed based on simulations. From the back-to-back measurement a one-way insertion loss of about 3 dB is determined. This does not include the estimated antenna efficiency losses of about 3 dB.

REFERENCES

- [1] E. Seler, M. Wojnowski, W. Hartner, J. Bock, R. Lachner, R. Weigel, and A. Hagelauer, "3D rectangular waveguide integrated in embedded wafer level ball grid array (eWLB) package," in *IEEE Electronic Components and Technology Conference (ECTC)*, pp. 956–962, May 2014.
- [2] C. Schmid, A. Fischer, R. Feger, and A. Stelzer, "A 77-GHz FMCW radar transceiver MMIC/waveguide integration approach," in *IEEE MTT-S International Microwave Symposium Digest (IMS)*, pp. 1–4, June 2013.
- [3] S. Jameson and E. Socher, "A wide-band CMOS to waveguide transition at mm-wave frequencies with wire-bonds," *IEEE Transactions on Microwave Theory and Techniques*, vol. 63, no. 9, pp. 2741–2750, September 2015.
- [4] X.-D. Deng, Y. Li, W. Wu, and Y.-Z. Xiong, "A D-band chip-to-waveguide-horn (CWH) antenna with 18.9 dBi gain using CMOS technology," in *IEEE International Wireless Symposium (IWS)*, pp. 1–4, March 2015.
- [5] J. Hasch, U. Wostradowski, S. Gaier, and T. Hansen, "77 GHz radar transceiver with dual integrated antenna elements," in *German Microwave Conference (GeMIC)*, pp. 280–283, March 2010.
- [6] M. Hitzler and C. Waldschmidt, "Design and characterization concepts of a broadband chip-integrated antenna," in *European Microwave Conference (EuMC)*, pp. 96–99, October 2014.
- [7] R. Alhalabi and G. Rebeiz, "Design of high-efficiency millimeter-wave microstrip antennas for silicon RFIC applications," in *IEEE Inter. Symp. on Antennas and Propagation (APSURSI)*, pp. 2055–2058, July 2011.
- [8] A. Hofmann, E. Horster, J. Weinzierl, L. Schmidt, and H. Brand, "Flexible low-loss dielectric waveguides for THz frequencies with transitions to metal waveguides," in *European Microwave Conference (EuMC)*, pp. 955–958, October 2003.